

Available online at [www.sciencedirect.com](http://www.sciencedirect.com)

SCIENCE @ DIRECT®

Developmental Biology 290 (2006) 411–420

DEVELOPMENTAL  
BIOLOGY[www.elsevier.com/locate/ydbio](http://www.elsevier.com/locate/ydbio)

## Dystroglycan is required for proper retinal layering

Andrea Lunardi<sup>a,1</sup>, Federico Cremisi<sup>b</sup>, Luciana Dente<sup>a,\*</sup>

<sup>a</sup> *Dipartimento di Fisiologia e Biochimica, Laboratori di Biologia Cellulare e dello Sviluppo, Università di Pisa, via G. Carducci 13, Ghezzano, Pisa 56010, Italy*

<sup>b</sup> *Scuola Normale Superiore di Pisa, piazza dei Cavalieri 7, 56100 Pisa, Italy*

Received for publication 2 March 2005, revised 5 September 2005, accepted 30 November 2005

Available online 9 January 2006

### Abstract

Dystroglycan (DG) is a transmembrane receptor linking the extracellular matrix to the internal cytoskeleton. Its structural function has been mainly characterized in muscle fibers, but DG plays signaling and developmental roles also in different tissues and cell types. We have investigated the effects of dystroglycan depletion during eye development of *Xenopus laevis*. We have injected a specific morpholino (Mo) antisense oligonucleotide in the animal pole of one dorsal blastomere of embryos at four cells stage. Mo-mediated loss of DG function caused disruption of the basal lamina layers, increased apoptosis and reduction of the expression domains of specific retinal markers, at early stages. Later in development, morphants displayed unilateral ocular malformations, such as microphthalmia and retinal layering with photoreceptors and ganglion cells scattered throughout the retina or aggregated in rosette-like structures. These results recall the phenotypes observed in specific human diseases and suggest that DG presence is crucial at early stages for the organization of retinal architecture.

© 2005 Elsevier Inc. All rights reserved.

**Keywords:** Dystroglycan; Retinal development; Layering; Basal lamina; Morpholino oligonucleotide; *Xenopus* expression pattern

### Introduction

Dystroglycan (DG) is a central component of the dystrophin-associated protein complex (DAP) that is deeply disorganized in muscles of patients with congenital muscular dystrophies. Damage of muscle fibers is often associated with ophthalmic and central nervous system anomalies in severe forms of disease, such as Duchenne Muscular Dystrophy, where mutations of the dystrophin gene lead to destabilization of the DAP complex. In different tissues, distinct variants of DAP complexes are present, but in each case, DG is always the principal receptor, playing the important role of linking extracellular matrix (ECM) proteins to intracellular cytoskeleton (Winder, 2001).

Patients with other congenital muscular dystrophies, such as Walker–Warburg syndrome (WWS), muscle–eye–brain (MEB) disease, Fukuyama congenital muscular dystrophy (FCMD), also suffer from muscular dystrophy, eye abnormal-

ities and CNS neuronal migration defects (Dubowitz, 2000; Hayashi et al., 2001; Kano et al., 2002; Michele et al., 2002; Toda et al., 2000). In this group of diseases, specific glycosyltransferase enzymes are affected and DG is hypoglycosylated (Muntoni et al., 2002). Indeed, proper glycosylation of DG is essential for specific binding to a variety of ECM proteins such as laminin, agrin or perlecan (Endo and Toda, 2003) (Toda et al., 2000).

DG is produced as a precursor polypeptide that is processed into two interacting  $\alpha$  and  $\beta$  subunits.  $\alpha$ -DG is extracellular and is extensively glycosylated in a tissue-specific manner,  $\beta$ -DG is a transmembrane protein that binds to dystrophin and other intracellular proteins (Winder, 2001). Alterations of the glycosylation pattern impair the function of  $\alpha$ -DG in binding to ECM proteins and, as a consequence, influences signal transduction and connection to cytoskeletal proteins mediated by  $\beta$ -DG. Animal models, such as *myd*<sup>Large</sup> mice, where DG glycosylation carried out by Large protein was impaired, showed similarities to the heterogeneous group of human muscle–eye–brain diseases listed above (Kanagawa et al., 2004; Michele et al., 2002).

Furthermore, targeted DG depletion in mouse brain provoked even more severe pathological features, including

\* Corresponding author. Fax: +39 50 878486.

E-mail address: [dente@dfb.unipi.it](mailto:dente@dfb.unipi.it) (L. Dente).

<sup>1</sup> Current address: Laboratorio Nazionale CIB, Area Science Park, Padriciano 99, 34012 Trieste, Italy.

disarray of cerebral cortical layering, lissencephaly and aberrant migration of granule cells, associated with loss of ability to organize the basal lamina of the glia limitans (Moore et al., 2002). On the other hand, full removal of DG in knockout mice resulted in embryonic death, because assembly of pivotal basement membrane (Reichert's membrane) was impaired (Williamson et al., 1997).

All these data, and others that directly prove DG involvement in basal laminae assembly, strongly support a crucial role for DG in early development and in the morphogenesis of neuroepithelial tissues. The vertebrate retina is part of the central nervous system (CNS) and like other CNS structures is characterized by a layered architecture containing distinct cell types. Therefore, it is a useful model to study mechanisms of CNS differentiation and morphogenesis. In this work, we have investigated the function of DG during *Xenopus laevis* retinogenesis, focusing on the effects of its depletion since early developmental stages. Loss of DG function in the eye, mediated by DG-specific morpholino oligonucleotides, leads to ocular malformations including microphthalmia, retinal delayering and clustering of rosette-like structures that resemble typical features of human muscle–eye–brain diseases.

## Material and methods

### *Xenopus laevis* embryos

*Xenopus* females were preinjected with 100 U of pregnant mare serum gonadotrophin (Folligon, Intervet) 4–11 days prior to egg collection and with 800–1000 U of human chorionic gonadotrophin (Profase HP 2000, Serono) the night before collection. Ovulated eggs were fertilized with testis homogenates and allowed to develop in 0.1 XMMR (1 XMMR is 0.1 M NaCl, 2 mM KCl, 1 mM MgSO<sub>4</sub>, 2 mM CaCl<sub>2</sub>, 5 mM HEPES, 0.1 mM EDTA). Jelly coats were removed in 3.2 mM DTT, 0.2 M Tris pH 8.8. Embryos were staged according to the Nieuwkoop and Faber-*Xenopus* table (Nieuwkoop and Faber, 1967).

### In situ hybridization

Whole-mount in situ hybridization experiments on *Xenopus* embryos were carried out as described by (Harland, 1991). Standard cRNA synthesis from linearized plasmids using SP6, T7 or T3 RNA polymerases were carried out incorporating digoxigenin (DIG) substituted ribonucleotides. The following probes were used: *X-DG* (Lunardi and Dente, 2002); *Xrx1* (Casarosa et al., 1997); *Xotx2* (Pannese et al., 1995); *Xotx5* (Vicizian et al., 2003); *β-crystallin* (Altmann et al., 1997); *hermes* (Gerber et al., 1999). In situ hybridization on sections was performed as described by Vicizian et al. (2003). Histological examinations were performed as described in Pannese et al. (1995).

### Immunohistochemistry

*Xenopus* embryos were fixed for 1 h in 4% paraformaldehyde in 100 mM phosphate buffer pH 7.4, then cryoprotected by immersion in 25% sucrose overnight at 4°C. Tissues were frozen in freezing medium (OCT compound; Sakura Finetek Europe B.V.), sectioned at 12 μm thickness in a cryostat, collected on slides (Superfrost Plus; Menzel Glaser Germany), air dried for 30 min and finally stored at –80°C until use. Before the onset of the immunohistochemistry procedure, sections were defrosted and blocked for 1 h at room temperature in PBS pH 7.4, 10%, inactivated lamb serum and 0.5% Triton X-100. Sections were incubated overnight at 4°C in PBS supplemented with 3% NGS (normal goat serum) and 0.5% Triton X-100. The primary antibodies used were mouse anti-dystroglycan (43DAG/8D5, Novocastra diluted 1:50), mouse anti-acetylated-tubulin antibody (SIGMA T6793 diluted 1:500), mouse anti-β-1 integrin (8C8, purchased from Developmental Studies

Hybridoma Bank, University of Iowa, Iowa City, IA diluted 1:10), rabbit anti-laminin (SIGMA L-9393, diluted 1: 400), rabbit anti aPKC (Santa Cruz Biotechnology C-20, Sc-216, diluted 1:1000). After washing in PBS, 0.2% Tween 20, incubation with appropriate secondary antibodies was performed: sheep anti-mouse antibody CY3 conjugated (SIGMA C2181, diluted 1:200) or FITC conjugated (SIGMA F2883, 1:100) anti-rabbit. Nuclei were labeled with Hoechst 33258 (SIGMA diluted 1:1000 in PBS). Slides were washed and mounted using Aqua Poly/Mount (polisciences Inc.).

### Morpholino microinjection

A specific antisense morpholino oligonucleotide (Mo-X-DG) was designed against the 5' sequence upstream to the DG start codon of translation: 5'-TACAGCGTAGGAGGCAGCTTGTCT-3'. Gene Tools Mo-standard (5'-CCTCTTACCTCAGTTACAATTTATA-3') was used for control morpholino injections. Microinjections were performed using a Drummond "Nanoject" apparatus. *Xenopus* embryos were injected in 0.1 XMMR and 4% Ficoll 400, and cultured overnight at 14°C in the same solution. Embryos were subsequently transferred to 0.1 XMMR and grown at RT until they reached the desired stage. Morpholino oligos were injected in a volume of 10 nl into the dorsal animal pole of one of the four blastomeres in the following amounts: 17, 8, 4 and 2 ng of Mo-X-DG; 17 ng of Mo-standard (Gene Tools). 250 pg of either green fluorescent protein or β-galactosidase RNA was co-injected with Morpholino oligo to visualize the injected side of the embryos. When β-galactosidase (β-gal) RNA was used as tracer, the embryos were fixed in MEMFA for 1 h at RT, washed in 0.1 M phosphate buffer pH 6.3, and the stained in a solution containing 32.93 mg potassium ferricyanide, 42.24 mg potassium ferrocyanide, 15 mg salmon-Gal substrate (Roche) in 10 ml of phosphate buffer pH6.3, for 5–60 min at 37°C. Embryos were then gradually dehydrated with ethanol and subjected to histological examination or whole-mount in situ hybridization.

### BrdU assay

BrdU (10 mg/ml) was administered for 2 h by intra-abdominal microinjection (50 nl) in stage 30 embryos. Eye cryosections (12 μm) were treated with 2 N HCl (20' at RT), buffered with 5 PBS washes (3' each) and immunostained with anti-BrdU antibody (Sigma, 1:500). The proportion of the nuclei (visualized by Hoechst staining) that incorporated BrdU (detected by sheep anti-mouse antibody CY3) was analyzed in both sides of 25 embryos injected unilaterally with DGMo at 4 cell stage.

### TUNEL assay

Stage 30–32 embryos were fixed in 4% PFA 45' at RT and embedded for cryostat sectioning. To stain apoptotic cell nuclei, we used the ApopTag Peroxidase Kit (Serologicals), following the manufacturer's instruction. TUNEL-positive cells were counted in eye sections of the injected and control sides of 30 DGMo-injected embryos.

## Results

### Dystroglycan expression during eye development

We have previously described the pattern of DG spatio-temporal expression in *X. laevis* embryos (Lunardi and Dente, 2002). Using an antisense probe for α-β dystroglycan precursor for in situ hybridization analysis, we detected early presence of *Xenopus* DG (X-DG) mRNA in a variety of tissues and cell types of different embryological derivation. In the present study, we have focused our analysis on DG specific expression in the eye at different developmental stages.

Embryos were analyzed using whole-mount in situ hybridization and subsequent histological sectioning (Fig. 1). At

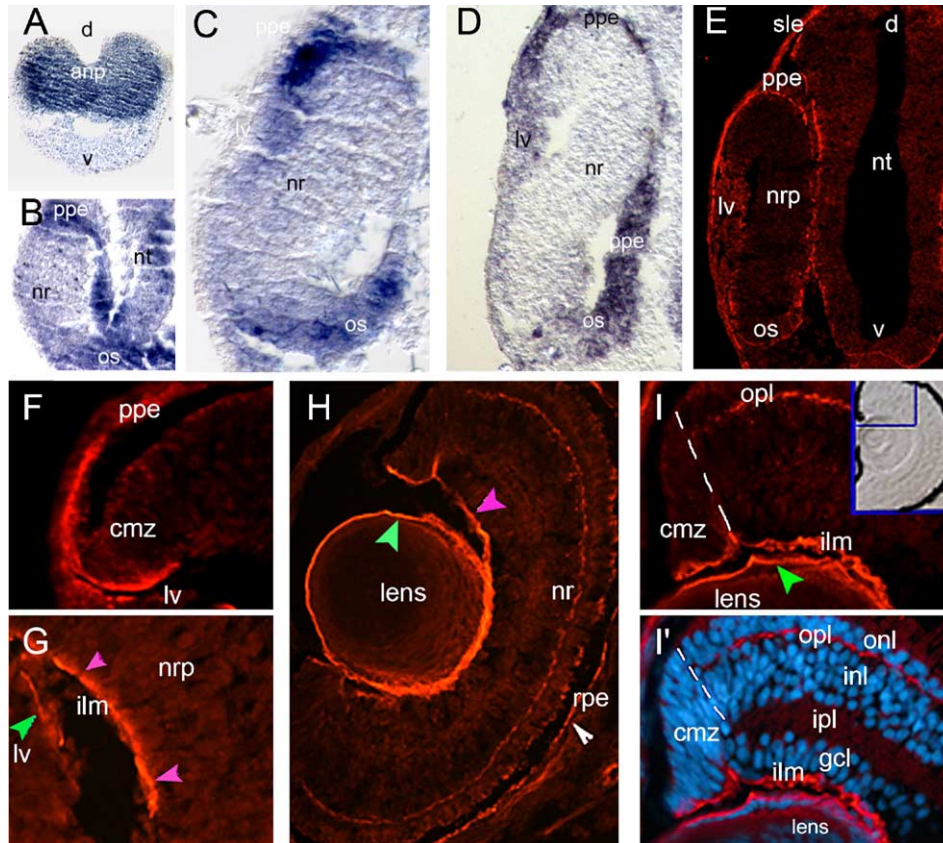


Fig. 1. Dystroglycan gene expression during early *Xenopus laevis* retinogenesis. Panels A–D are sections of in situ whole-mount hybridized embryos from stage 19 to stage 28. (A) Tangential section showing DG mRNA expression localized in the anterior neural plate at stage 19. (B–D) Transversal sections showing X-DG mRNA expression at stage 24 (B), at stage 26 (C) and at stage 28 (D) in the optic stalk, in the presumptive pigmented epithelium and in the lens vesicle (C, D). Panels E–I' are cryostat sections showing X-DG immunolocalization. (E) X-DG detection at stage 28 in the neural tube and in the retina at the level of the presumptive pigmented epithelium, the optic stalk and all around the sensorial layer of the ectoderm. (F, G) High magnification of retina sections at stage 32 showing the presence of X-DG in the endfeet of retinal precursors in the ciliary marginal zone and in the inner limiting membrane at the vitreal border of the retina (purple arrowheads in panel G). Green arrowheads indicate X-DG detection in the lens vesicle. (H–I') Transverse sections of *Xenopus* retina at stage 45 showing X-DG immunoreactivity at the level of retinal pigmented epithelium (white arrowhead), inner limiting membrane (purple arrowhead) and lens epithelium (green arrowhead). Punctuated distribution of X-DG in the OPL is evidenced at high magnification in panels I, I' (same section, red detection) between the two nuclear layers, highlighted in panel I' by Hoechst staining. Abbreviations: anp, anterior neural plate; OS, optic stalk; ppe, presumptive pigmented epithelium; nr, neural retina; nrp, neural progenitors; lv, lens vesicle; d, dorsal; v, ventral; nt, neural tube; sle, sensorial layer of ectoderm; cmz, ciliary marginal zone; gcl, ganglion cell layer; inl, inner nuclear layer; onl, outer nuclear layer; opl, outer plexiform layer; ipl, inner plexiform layer; ilm, inner limiting membrane.

neurula stage (stage 19; Fig. 1A), X-DG mRNA was spread throughout a wide area in the anterior neural plate, which includes the prospective eye field with the neural retinal progenitors. At the early tailbud stage (stage 25; Fig. 1B) DG mRNA expression was concentrated at level of the optic stalk and of the presumptive pigmented epithelium. Later (stages 26–28; Figs. 1C, D), when the neural layer of the eye vesicle begins to bend inwards to form the eye cup, X-DG expression started to be detectable also in the lens vesicle.

Detection of X-DG protein at these early stages was difficult. In contrast, from stage 28 to stage 45, its distribution could be revealed by immunohistochemistry on cryostat sections, using the antibody 43DAG/8D5. This antibody recognizes the  $\beta$ -DG carboxy-terminus, a region highly conserved in most vertebrate species, *Xenopus* included (Lunardi and Dente, 2002). At tailbud stage (st.28), specific immunoreactivity was detectable in the presumptive pigmented epithelium, in the optic stalk and in the sensorial layer of the ectoderm (Fig. 1E). Starting from stage 32, it was possible to

localize X-DG protein in the vitreal border of the retina, at the level of the endfeet of the retinal precursor cells (high magnification in Figs. 1F, G) and in the lens vesicle (Fig. 1G). At stage 45, when the *Xenopus* retina is fully differentiated, a distribution similar to the pattern already described in several other vertebrate retinas was found (reviewed in Schmitz and Drenckhahn, 1997). A strong and continuous immunoreactivity was evident at level of lens epithelium and of the inner limiting membrane (Figs. 1H–I'). Weaker but reproducible immunosignal was present as a punctate line in the outer plexiform layer (Figs. 1I, I'). The same punctate DG immunolocalization has been shown to correspond to specific synaptic complexes in bovine, rat and mouse retinas (Blank et al., 1997, 1999; Koulen et al., 1998).

#### Loss of dystroglycan function

Our analysis revealed presence of X-DG protein during the early steps of eye retinogenesis in the neuroepithelium,

pigmented epithelium and lens progenitors. An obvious question is whether X-DG was involved in the morphogenetic processes taking place at this time. To address this question, we used an approach of “morpholino-mediated targeted depletion” (Heasman, 2002). We designed a specific antisense morpholino oligonucleotide (Mo-X-DG), complementary to the 5' end of the X-DG transcript and fit to interfere with DG translation. In order to avoid lethal effects deriving from a widespread dystroglycan loss of function and to focus the analysis at eye level, we injected Mo-XDG at the animal pole of one dorsal blastomere, at four cells stage. In fact, this injected cell generates one half of the anterior aspect of nervous system, including the eye. The uninjected half of the embryo represents the internal control of the experiment.

Mo-X-DG (17 ng, 8 ng, 4 ng and 2 ng) was injected in combination with 250 pg of  $\beta$ -gal ( $\beta$ -galactosidase) or GFP (green fluorescent protein) RNA, as tracers to analyze the resulting phenotypes.

Direct analysis of the effect on X-DG protein by immunohistochemistry showed that the injection of 8 ng of Mo-X-DG was sufficient to prevent dystroglycan translation (Fig. 2). Absence of DG immunoreactivity was found in the injected side and in rare cells of the other side, only when diffusion of the injected material was sporadically observed (Figs. 2B, C).

Stage 45 embryos, injected with 17 ng of Mo-X-DG, showed strong anterior malformations (data not shown) either in the injected or uninjected sides (88%; number of morphants,  $n = 82$ ). In contrast, embryos injected with 8 ng of Mo-X-DG exhibited microphthalmia only in the injected side (82%,  $n = 111$ ) (Fig. 2A). The injection of 4 ng showed a consistent reduction of embryos with microphthalmia (30%,  $n = 110$ ), while no altered phenotypes were found in embryos injected with 2 ng ( $n = 60$ ). In Morpholino toxicity test, identical doses of a standard Morpholino oligonucleotide (Gene Tools) were injected: only few embryos showed anterior defects (3%,  $n = 235$ ).

#### *Early phase of development: phenotypic effects of dystroglycan depletion*

Mo-mediated inactivation of X-DG produced a general reduction of the eye size, as evaluated by external morphological analysis of the morphants. In principle, X-DG depletion could exert this effect by affecting the expression of genes that pattern the eye field during early development. To address this point, we analyzed the expression of three genes whose early expression identifies different eye domains. *Xrx1* is an eye master gene that is expressed in the eye field region of the anterior neural plate starting from stage 13 and marks neural retina progenitors throughout all retinal development (Andreazzoli et al., 1999; Casarosa et al., 1997). *Xotx2* is a marker of developing forebrain structures, including the eye. Its expression domain surrounds that of *Xrx1* in the early developing eye (stage 13/15) (Andreazzoli et al., 1999; Kablar et al., 1996; Pannese et al., 1995), and later (stage 25/33) it marks the undifferentiated neural retina (Vicizian et al., 2003).  $\beta$ -Crystallin is an early marker of the lens (Altmann et al., 1997).

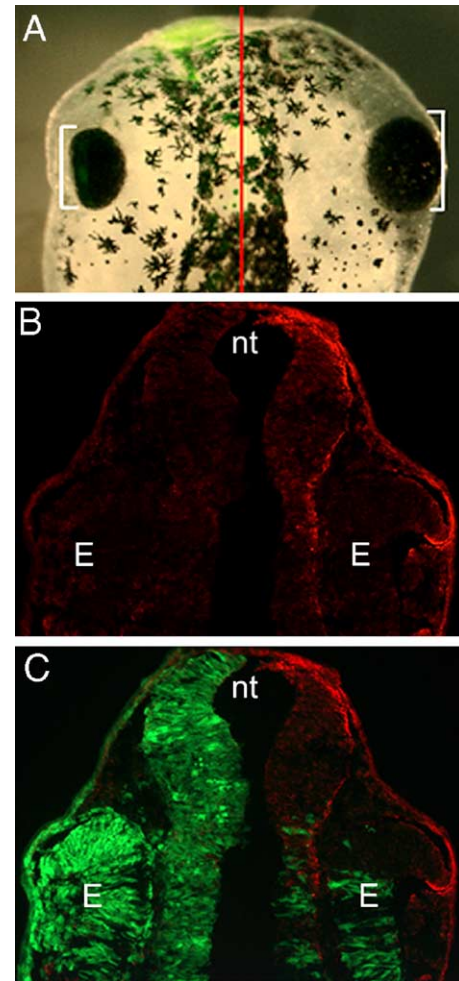


Fig. 2. Results of DG loss-of-function experiments. (A) Stage 45 *Xenopus* embryo injected at four cells stage with 8 ng of Mo-X-DG plus 250 pg of GFP cRNA. The injected side is indicated by the green staining; white brackets highlight reduction of the eye size in the injected side (left) compared to the uninjected, control side (right). (B, C) Transversal section of a stage 32 injected embryo in which specific DG immunostaining (in red) is lost in neural tube (nt) and eye (E) of the Mo-X-DG-injected side and in some cells of the other side, where diffusion of the injected material sporadically happens. Fluorescent green labeling shows the injected side of the embryo in panel C.

Comparison of the expression pattern of *Xrx1*, *Xotx2* and  $\beta$ -crystallin mRNA in Mo-X-DG-injected embryos is shown in Fig. 3. *Xotx2* and *Xrx1* markers labeled their respective domains in the injected side as well as in the control side at stage 14, thus suggesting that Mo-mediated X-DG inactivation did not affect the early induction of the eye field (*Xotx2*,  $n = 27$ ; *Xrx1*,  $n = 45$ ; Figs. 3A, B). However, starting from stage 25 (*Xotx2*, 66%  $n = 30$ ; *Xrx1*, 59%,  $n = 85$ ; Figs. 3C, D) and later at stage 28 (*Xotx2*, 85%  $n = 33$ ; *Xrx1*, 87%,  $n = 72$ ; Figs. 3E–G'), DG depletion caused a significant reduction of the expression domains of either *Xotx2* (Figs. 3C, E, E') *Xrx1* (Figs. 3D, F, F'), and  $\beta$ -crystallin (87%,  $n = 48$ ; Figs. 3G, G') in the injected side.

DG is a transmembrane receptor that plays an active role during the assembly of specific basement membranes, and it is supposed to mediate signal transduction from the ECM (Henry and Campbell, 1998). To verify the effects of DG depletion on basement membranes of *Xenopus* eye, cryostat sections of the

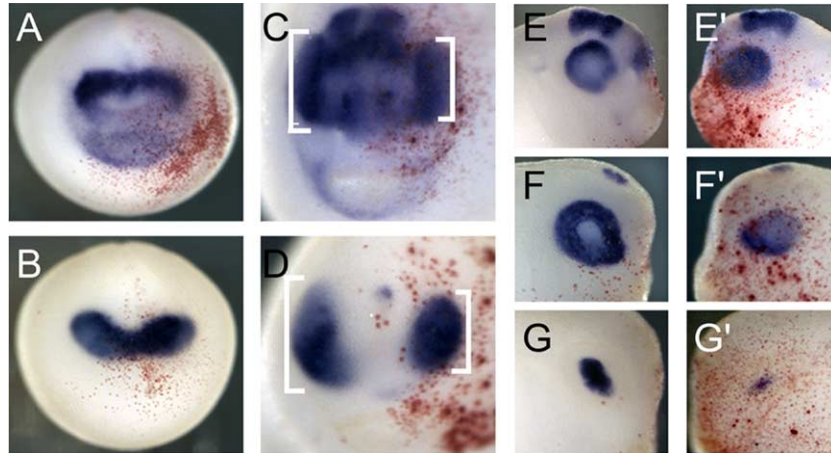


Fig. 3. Expression of eye markers in X-DG morphants. *Xotx2* (A, C, E, E'), *Xrx1* (B, D, F, F') and  $\beta$ -crystallin (G, G') mRNA expression was detected by BMP purple (blue staining) in Mo-X-DG-injected embryos at stage 14 (A, B), 25 (C, D) and 28 (E–G'). Nuclear beta-gal staining (red) was used to trace the side of injection. Panels A–D show both injected and uninjected sides in frontal views. Panels E–G' show lateral view of uninjected (E, F, G) and injected (E', F', G') sides, respectively. No changes in the expression domains of *Xotx2* (A) and *Xrx1* (B) are detectable between the two sides at stage 14. White brackets highlight the decrease of *Xotx2* (C) and *Xrx1* (D) expression in the eye of the injected sides at stage 25. Decrease is evident also at stage 28 (compare panel E to E' and F to F');  $\beta$ -crystallin expression is also dramatically reduced in the injected side (compare panel G to G'). Mo-X-DG injection completely abolishes also *Xotx2* rostral expression domain in panels E to E'.

anterior region of morphants at stage 32 were analyzed by immunostaining with specific laminin and integrin antibodies (Fig. 4). The anti-laminin antibody used in this analysis

recognizes the heterotrimer Lam1 (including  $\alpha$  1,  $\beta$ 1,  $\gamma$ 1 subunits) that is present in the two main retinal basement membranes: the Bruch's membrane at the bases of pigmented

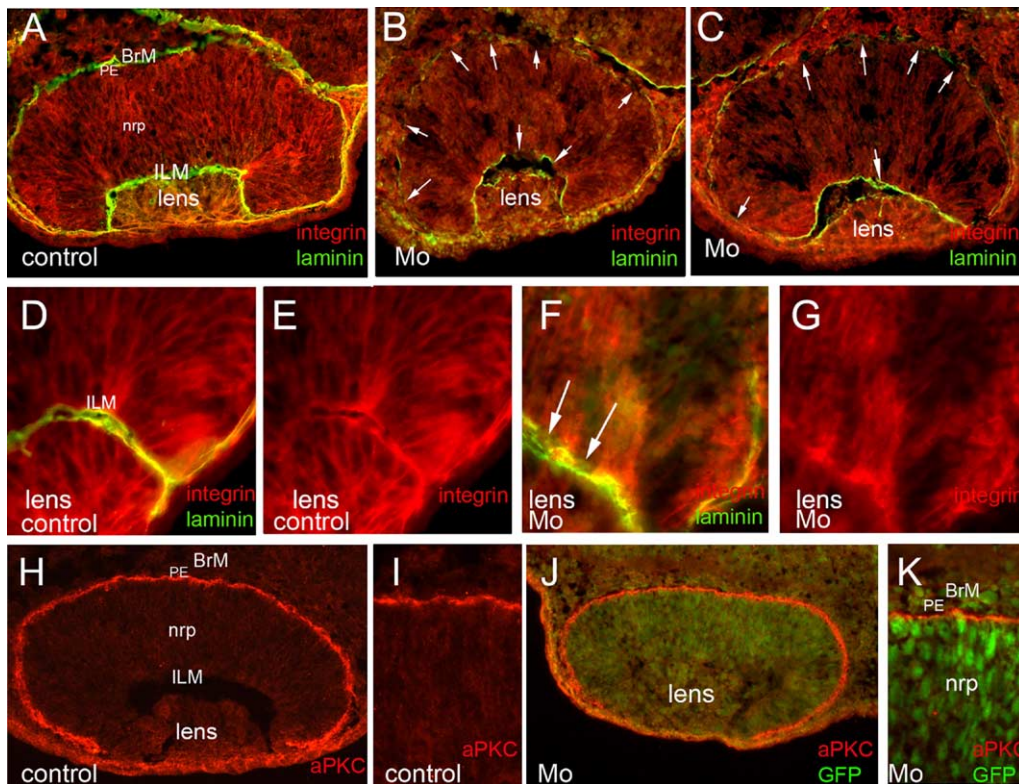


Fig. 4. Cryostat sections of *Xenopus* retina immunolabeled with polyclonal antibody against Lam1 (A–D and F: green labeling); monoclonal antibody against  $\beta$ 1-integrin (A–G: red labeling) and polyclonal antibody against aPKC (H–K: red labeling). Control side (A, D, E, H, I) and injected side (B, C, F, G, J, K) of retinas at stage 32. The injected side in panels J and K was traced by GFP. Laminin and integrin were co-detected (yellow signal) in the Bruch's membrane (BrM) at the bases of pigmented epithelium (PE), at the border of vitreal cavity in the inner limiting membrane (ILM) and in the lamina surrounding the lens. Severe disorganization of these laminae was detected in the injected sides of morphants (arrows in panels B, C, F). Integrin staining, which showed a radial-like pattern in the control sides (A, E) was affected in the injected sides of morphants (B, C, G). High magnifications (D–G) highlight the histology of the retina at its most marginal side near the lens. Localization of aPKC at the apical side of the retinal neural precursors (nrp), underneath the pigmented epithelium (PE) was visible either in control (H, I) or in Mo-injected eye (J, K). At higher magnification, the aPKC staining of retinas in the control (I) and injected (K) sides was comparable.

epithelium and the inner limiting membrane at border of vitreal cavity (Libby et al., 2000). The anti-integrin antibody 8C8 is specific for the  $\beta 1$ -integrin subunit, which spans the entire width of the retina along the neuroepithelial precursors and is especially abundant at the site of contact of the retinal inner limiting membrane (ILM), where it acts as a laminin receptor (Li and Sakaguchi, 2002; Li et al., 2004). In the injected side of X-DG morphants, a delocalization of laminin was evident in 75% of morphants ( $n = 60$ ). Figs. 4B and C show two examples of the phenotypes obtained after injection of 8 ng of Mo-X-DG, compared to control (Fig. 4A). Basement laminae that form continuous and discrete sheaths in the control side (Figs. 4A, D, E) were frequently disrupted and/or disorganized in the injected side (arrows in Figs. 4B, C, F, G), either between the lens vesicle and the retinal border or under the developing pigmented epithelium, at level of the Bruch's membrane. Furthermore,  $\beta 1$ -integrin immunoreactivity, detectable with a radial-like pattern at the control side (Figs. 4A, D, E), resulted disturbed in the contralateral, injected side (Figs. 4B, C, F, G), even if the analysis of a large number of sections showed that the total protein level was unvaried.

In order to verify if the polarity of neuroepithelial precursors was also altered, the localization of aPKC, a marker of apical side of embryonal epithelia, was analyzed using the antibody C-20 that is raised against both PKC  $\lambda$  and  $\zeta$  (Horn-Badovinac et al., 2001); aPKC resulted correctly localized at the apical side of the retina underneath the presumptive pigmented epithelium of all the morphants analyzed (Figs. 5H, K).

#### Late phase of development: phenotypic effects of dystroglycan depletion

At stage 45, when *Xenopus* eyes are fully developed, severe retinal morphological disorders were detected in the injected side of 43% of the morphants ( $n = 117$ ). Evaluation of the late effects was carried out using specific markers of the different retinal cell types (Gerber et al., 1999; Viczian et al., 2003). As previously reported, in the control side *Xotx5* expression marked photoreceptors and a sub-type of bipolar cells in the mature retina (Fig. 5A), *Xotx2* was expressed in bipolar cells (Fig. 5B) and *hermes* specifically identified ganglion cells in the GCL (Fig. 5C). Finally, nervous fibers of both OPL and IPL were revealed by immunostaining of acetylated-N-tubulin (Fig. 5D).

One of the most evident late effects of Mo-X-DG injection was the presence of “rosette-like structures” (green arrowheads in Figs. 5A'–D'), which were made of misplaced photoreceptors exposing their external segments inside the hollow space of the rosette. In Mo-X-DG morphants, these structures were highlighted by expression of *Xotx5*, which was detected outside the ONL (green arrowheads in Fig. 5A'). Delayering of Mo-X-DG retinas was also confirmed by the pattern of *Xotx2* labeling (Fig. 5B'), which was dramatically disturbed compared to control retinas (Fig. 5B). In addition to photoreceptors and bipolar cells, ganglion cells were also misplaced, even if less frequently: in 30% ( $n = 117$ ) of the Mo-X-DG retinas, *hermes* was detected under the pigmented epithelium (red arrowhead in Fig. 5C') and/or near the rosette-like structures (not shown). Nonetheless, neuronal differentiation

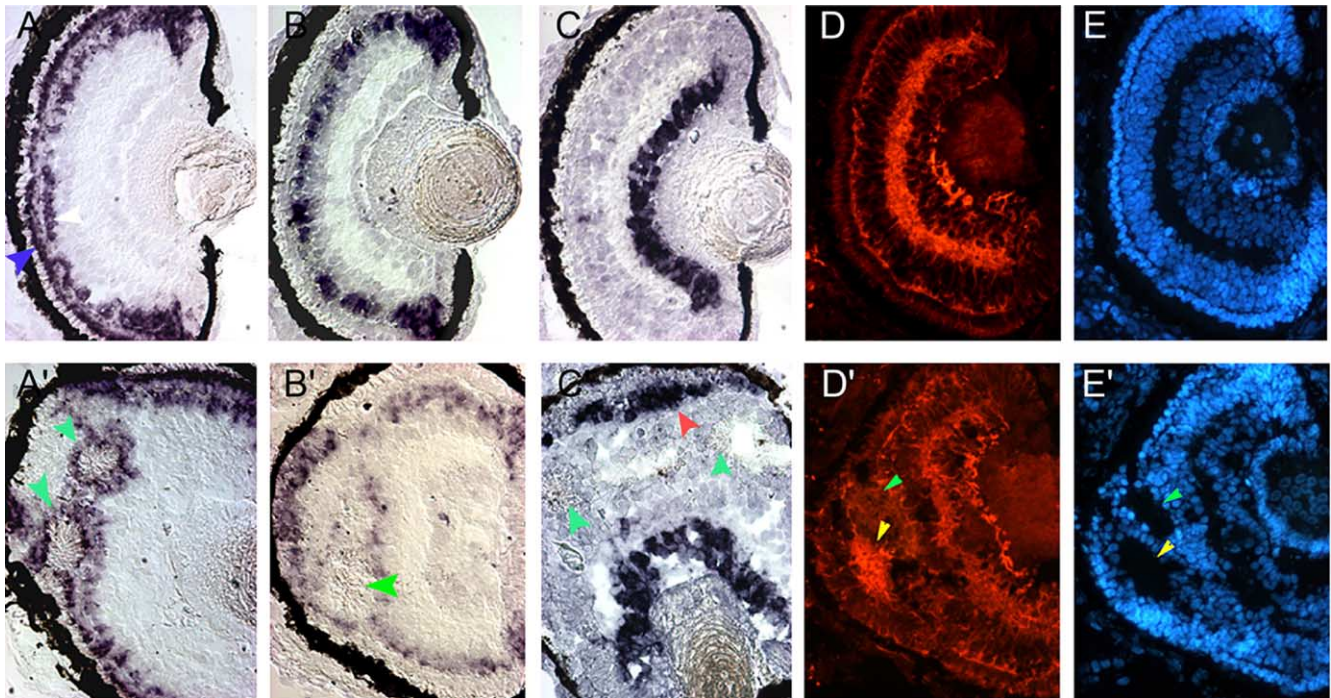


Fig. 5. Retinal delayering in DG morphants. (A–E) control sides; (A'–E') Mo-X-DG-injected sides. Expression of markers for specific cell types in retinal sections from stage 45 embryos: (A, A') *Xotx5* mRNA; (B, B') *Xotx2* mRNA; (C, C') *hermes* mRNA; (D, D') N-tubulin. (E, E') Hoechst nuclear staining of sections shown in panels D and D'. In panel A, blue and white arrowheads indicate photoreceptors and bipolar cells. Green arrowheads show rosette-like structures. Red arrowhead indicates ectopic *hermes* expression in panel C'. Yellow arrowheads indicate ectopic nervous fibers in panel D' and the corresponding position in panel E'.

of distinct cell types seemed not affected by Mo-X-DG injection. Nervous fibers were detected by immunostaining with acetylated-N-tubulin in Mo-X-DG retinas (Fig. 5D'), even if their pattern was dramatically disorganized when compared to controls (Fig. 5D). Notably, migration of retinal neuronal cells was altered: ectopic nervous fibers (as those indicated by yellow arrowhead in Fig. 5D') were often found close to rosette-like structures (green arrowhead) and near misplaced *hermes* positive cells (not shown).

## Discussion

The role of DG has been extensively studied in muscles, in view of its association to dystrophin and the involvement in muscular dystrophies. Recently, several findings have revealed a previously unrecognized role for DG in early events of neurogenesis, in migration and targeting of cell surface proteins that give plausible explanations of the histopathological neural features frequently present in congenital muscular dystrophies (Michele et al., 2002; Moore et al., 2002). Mental deficits are often coupled to ocular defects, such as retinal dysplasia with detachment and delayering, microphthalmia and cataract (Dubowitz, 2000; Hino et al., 2001; Kano et al., 2002; Toda et al., 2000).

In order to investigate the role of DG and the effects of its depletion during vertebrate eye development, we have first characterized its expression pattern in the embryonic and adult *Xenopus* eyes. We found that X-DG mRNA is already detectable at neurula stage in the eye field and later at tailbud stage, it is mainly concentrated in presumptive pigmented epithelium, in developing retina, in lens vesicle and optic stalk. Immunostaining of X-DG protein was detectable, at tailbud stage, as a concentrated signal on lens vesicle, on the vitreal border of the retina in the endfeet of neuroepithelial progenitors and on cells fated to form the pigmented epithelial layer in front to Bruch's membrane. Early expression of DG protein in the endfeet of neuroepithelial progenitors has been also observed in embryonic avian retina at stages preceding the differentiation of neurons or glial cells (Blank et al., 2002). This observation and the joined presence of other DAP components (i.e., dystrophin) lead the authors to suppose that DG could play a role in the developing retina similar to that well characterized in muscle (Blank et al., 2002; Schmitz and Drenckhahn, 1997). Beyond this structural role, later in the adult retina, DG is supposed to be involved in visual signal transduction. This is assumed on the bases of its specific localization in the finger-like extensions protruding from photoreceptors (Blank et al., 1997, 1999; Koulen et al., 1998). Indeed, we found that DG protein distribution in fully differentiated *Xenopus* eye (stage 45) was similar to the pattern described in other vertebrate species (Blank et al., 1997, 1999; Koulen et al., 1998). DG immunoreactivity appeared as a punctate staining in correspondence of the OPL, while it was mainly concentrated, as a continuous layer, at the level of ILM, lens and retinal pigmented epithelium.

To gain more insight into the role of DG in the retina, we targeted morpholino-mediated DG depletion to the anterior

embryonic nervous system. The absence of DG immunoreactivity in the Mo-injected side of the embryos proved the blocking effect of morpholino injection on DG protein production. A main morphological effect of DG depletion was microphthalmia, which is an ophthalmological feature often described also in human CMD (Cormand et al., 2001; Hino et al., 2001). The precise mechanism that causes the eye size reduction has not been so far elucidated in this kind of diseases. In principle, the reduction of eye size could be exerted by different mechanisms, such as induction of a premature differentiation, reduced rate of proliferation of cell progenitors or induction of unscheduled apoptosis. To address these hypotheses, we investigated if deregulation of genes that pattern the eye field, such as *Xrx1* (Andreazzoli et al., 2003) or *Xotx2* (Zuber et al., 2003), was detectable in the injected side. In contrast, at stage 14, the expression pattern of both genes was unaffected, suggesting that DG depletion does not involve changes of identity of the early eye field. However, at later stages, a reduction of the expression domains of either *Xrx1*, *Xotx2* or  $\beta$ -*crystallin* was evident in the injected side. In order to distinguish if the reduction was due to diminished cell proliferation or increased apoptosis, we performed specific assays shown in Fig. 6. The number of injected cells (highlighted by the green GFP fluorescence), which incorporated BrdU and therefore were actively proliferating, was lower than the number detected in the control side, as expected considering the decrease of expression of *Xrx1*, a main determinant of the proliferation of retinal progenitors (Andreazzoli et al., 2003; Casarosa et al., 2003) (Figs. 6A, D). However, the difference between the two sides was lower than 10% (Fig. 6G) and cannot fully explain the marked microphthalmia associated to DG depletion. In contrast, the number of apoptotic cells, measured by TUNEL assay, was almost 10 times higher in the MO-injected side compared to the control side (Figs. 6E, F, H), suggesting that this is the mechanism deriving as secondary effect of the basal membranes (BM) disorganization.

Indeed, in addition to microphthalmia, two main phenotypes were associated to DG depletion. An early effect was the disorganization of the basal laminae of both retina and lens. A later effect consisted of a dramatic delayering of the neural retina. The two effects might be causally related. Severe perturbations of the ILM and of the Bruch's membrane were detected by analysis of the immunoreactivity to laminin-1 during early eye development. The two membranes were still present in the DG-depleted eyes at stage 32, but their structure was discontinuous and, in some cases, fainter compared to control.

DG and  $\beta$ 1-integrins are high affinity receptors of laminin-1, one of the main components of the ECM. DG and  $\beta$ 1-integrins bind to distinct region of the subunit  $\alpha$  of the laminin-1: the globular domains  $\alpha$ 1LG4-5 and  $\alpha$ 1LG1-3, respectively. These individual domains are supposed to play different roles in basal lamina organization and signaling (Ferletta et al., 2003; Henry et al., 2001; Scheele et al., 2005). In mouse embryonic stem cells, it has been shown that DG-laminin interaction was essential for the initial binding of laminin to cell surface; in

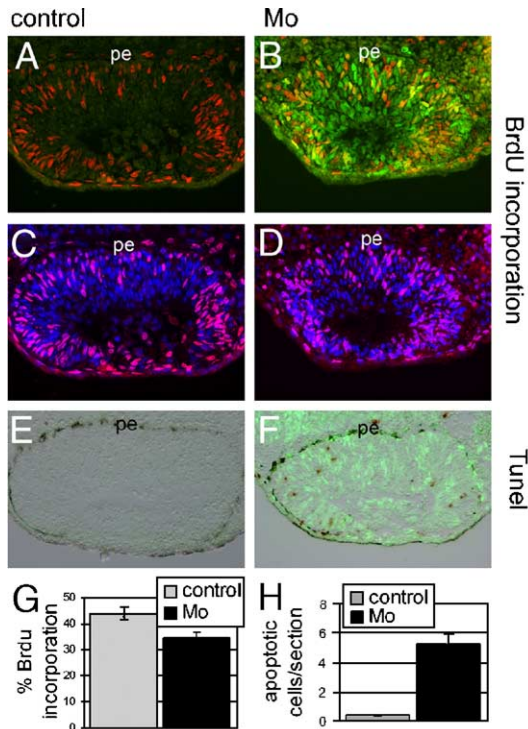


Fig. 6. Effects of the unilateral injection of Mo-X-DG (8 ng) at stage 4 cells on the apoptosis and cell proliferation of the eye. (A–F) Eye sections of stage 32 embryos. Pe: pigmented epithelium. Detection of GFP, which was used as tracer, is shown in panels B, D, F. Panels A–D show BrdU immunodetection (red nuclei) in the control side (A, C) and Mo-injected side (Mo, B, D) of the embryo. Hoechst counterstaining labels all nuclei in panels C, D. Panels E and F show TUNEL detection of apoptotic nuclei (brown staining) in control (E) and Mo-X-DG-injected side (F), respectively. Sections of Mo-X-DG injected eyes always displayed a significantly higher number of TUNEL-positive cells than sections of uninjected, contralateral eyes. Eyes injected with control-Mo had the same number of TUNEL-positive cells than uninjected eyes (not shown). The numbers of BrdU-positive nuclei in control and Mo-X-DG-injected (Mo) retinas, expressed as percent over the total number of cells analyzed (control:  $n = 550$ , Mo:  $n = 514$ ), are compared in panel G. The average number of TUNEL-positive cells per eye section ( $n = 120$  sections) in control and Mo-X-DG-injected retinas is compared in panel H. Bars indicate SE in panel G and SEM in panel H. Differences between control and Mo are significant in panel G ( $t$  test:  $P = 0.008904109$ ) and in panel H ( $t$  test:  $P = 8.997E-06$ ).

contrast,  $\beta$ 1-integrins were required for subsequent laminin-matrix assembly (Henry et al., 2001). On the other hand, in mice lacking only the DG/laminin binding domain  $\alpha$ 1LG4-5, the assembly of early basement membranes was normal, allowing embryos implantation, even if subsequent stem cells polarization and differentiation in epithelia failed (Scheele et al., 2005).

Basal laminae have established roles in correct development and differentiation of the epithelia. The distribution pattern of laminin-1 in the ILM and Bruch's membrane, observed in the injected side of X-DG morphants, suggests that DG presence is not essential for the assembly of these basal laminae; rather, DG seems important for maintaining the firm connections for ECM-cells adhesion. We speculate that the dramatic disorganization of the radial-like pattern of  $\beta$ -integrins in the DG-depleted eyes at stage 32 could be just caused by attenuation of ECM-cells adhesion.

A role of DG in supporting ECM-cells adhesion could be crucial for later retinal morphogenesis. Indeed, we have observed that absence of DG function, at early stages of *Xenopus* eye development, lead to consequent morphogenetic and histological alterations, later. The differentiation of distinct retinal cell types such as ganglion cells, photoreceptors and bipolar cells was not impaired in Mo-X-DG morphants, as assessed by hybridization with specific cell markers (*hermes*; *Xotx5*; *Xotx2*). In contrast, the layering of definite cell types was damaged by anomalous localization of photoreceptors and ganglion cells, which were scattered throughout the retina or aggregated in rosette-like structures.

Li and co-authors have recently shown analogous alterations in *Xenopus* retina, following perturbation of integrins function. Injection of  $\beta$ 1-integrin blocking antibodies or specific inhibitors into *Xenopus* optic vesicle, determined disruption of retinal development, rosette clustering with ectopic photoreceptors and retinal delayering (Li and Sakaguchi, 2004). Likewise, inhibition of BM adhesive function of  $\beta$ -integrins in embryonic chick neural retina determined alterations of cell morphology and increased apoptosis (Leu et al., 2004).

Finding comparable retinal phenotypes following inhibition of DG or integrin functions is not surprising, taking into account their common role in cell adhesion and ECM transduction signaling. Both receptors indeed, after ligand stimulation, induce phosphorylation of proteins on tyrosine residues (Lewis et al., 1996; Wary et al., 1998; James et al., 2000). Indeed, it has been shown that specific inhibition of protein tyrosine kinase activity in *Xenopus* retina altered cell adhesion and migration, causing disturbed retinal development (Li et al., 2004). Evidently, the correct attachment of the retinal progenitors at the BM is a crucial event that is controlled at multiple levels; it is sufficient to perturb one of the key components to severely interfere with the successive development steps.

Differentiation of retinal cell types is a complex process that starts at the time of cell cycle arrest, when most retinal cells start to migrate along polarized neuroepithelial progenitors to differentiate and form specific layers. Polarized precursors are essential to guide the cells to the right position. We may hypothesize that interruptions in the continuous sheath of laminins on retinal vitreal border and pigmented epithelium of X-DG morphants and the consequent detachment of retinal precursors from the BM could alter their migration. Ganglion cells are the first type to differentiate: they migrate from the apical side to the basal vitreal border of the retina, forming the ganglion cell layer. In fact, in a high percentage of X-DG morphants, ganglion cells were spread throughout the retina or remained at level of photoreceptors layer.

Genetic evidences deriving from a group of *zebrafish* mutants (*nok*, *has*, *ncad*) have suggested that loss of polarity of retinal precursors may affect the correct layering of retinal neurons (Pujic and Malicki, 2004). Furthermore, RNAi-mediated loss of function of a DG homolog protein in *Drosophila* resulted in expanded expression of some apical markers in progenitors of epithelial cells (Deng et al., 2003). In order to verify if perturbation of cell polarity was implicated in



Mo-generated phenotypes, we analyzed the distribution of aPKC, a typical apical marker (Horne-Badovinac et al., 2001). In *Xenopus* DG morphants, the apical polarity of neuroepithelial precursors cells was not significantly altered, as shown by the correct localization at the ventricular side of the embryonic retina of the apical marker aPKC (Figs. 5H, K).

Thus, these observations suggest that retinal delayering observed after DG depletion in *Xenopus* might be functionally related to weakening of cell adhesion to basal membranes, which in turn would impair the anchoring of retinal progenitors. This mechanism reminds that suggested in CNS<sup>DG-null</sup> or *myd*<sup>Large</sup> mice, where DG perturbation is associated to disruption of basal laminae, misplaced neurons and abnormal cortical cells layering (Michele et al., 2002; Moore et al., 2002). Our findings underscore the importance of DG in eye morphogenesis and allow to plan further use of *Xenopus* as model system for studying human diseases associated to affected DG.

### Acknowledgments

We would like to thank Ming Nam Liu for performing some experiments, G. Barsacchi and R. Vignali for their helpful discussion and M. Andreazzoli for the suggestions and careful reading of the manuscript. Thanks to M. Fabbri and G. De Matienzo for their technical assistance and S. De Maria for the frog's care. This work was supported by FIRB Neuroscienze (RBNE01 WY7P), by AMBISEN Center, Univ. Pisa, by MIUR-PRIN and by EC quality of life and management on living resources program (QLG3-CT-01460).

### References

- Altmann, C.R., Chow, R.L., Lang, R.A., Hemmati-Brivanlou, A., 1997. Lens induction by Pax-6 in *Xenopus laevis*. *Dev. Biol.* 185, 119–123.
- Andreazzoli, M., Gestri, G., Angeloni, D., Menna, E., Barsacchi, G., 1999. Role of Xrx1 in *Xenopus* eye and anterior brain development. *Development* 126, 2451–2460.
- Andreazzoli, M., Gestri, G., Cremisi, F., Casarosa, S., Dawid, I.B., Barsacchi, G., 2003. Xrx1 controls proliferation and neurogenesis in *Xenopus* anterior neural plate. *Development* 130, 5143–5154.
- Blank, M., Koulen, P., Kroger, S., 1997. Subcellular concentration of beta-dystroglycan in photoreceptors and glial cells of the chick retina. *J. Comp. Neurol.* 389, 668–678.
- Blank, M., Koulen, P., Blake, D.J., Kroger, S., 1999. Dystrophin and beta-dystroglycan in photoreceptor terminals from normal and *mdx3Cv* mouse retinae. *Eur. J. Neurosci.* 11, 2121–2133.
- Blank, M., Blake, D.J., Kroger, S., 2002. Molecular diversity of the dystrophin-like protein complex in the developing and adult avian retina. *Neuroscience* 111, 259–273.
- Casarosa, S., Andreazzoli, M., Simeone, A., Barsacchi, G., 1997. Xrx1, a novel *Xenopus* homeobox gene expressed during eye and pineal gland development. *Mech. Dev.* 61, 187–198.
- Casarosa, S., Amato, M.A., Andreazzoli, M., Gestri, G., Barsacchi, G., Cremisi, F., 2003. Xrx1 controls proliferation and multipotency of retinal progenitors. *Mol. Cell. Neurosci.* 22, 25–36.
- Cormand, B., Pihko, H., Bayes, M., Valanne, L., Santavuori, P., Talim, B., Gershoni-Baruch, R., Ahmad, A., van Bokhoven, H., Brunner, H.G., Voit, T., Topaloglu, H., Dobyns, W.B., Lehesjoki, A.E., 2001. Clinical and genetic distinction between Walker–Warburg syndrome and muscle–eye–brain disease. *Neurology* 56, 1059–1069.
- Deng, W.M., Schneider, M., Frock, R., Castillejo Lopez, C., Gaman, E.A., Baumgartner, S., Ruohola-Baker, H., 2003. Dystroglycan is required for polarizing the epithelial cells and the oocyte in *Drosophila*. *Development* 130, 173–184.
- Dubowitz, V., 2000. Congenital muscular dystrophy: an expanding clinical syndrome. *Ann. Neurol.* 47, 143–144.
- Endo, T., Toda, T., 2003. Glycosylation in congenital muscular dystrophies. *Biol. Pharm. Bull.* 26, 1641–1647.
- Ferletta, M., Kikkawa, Y., Yu, H., Talts, J.F., Durbeej, M., Sonnenberg, A., Timpl, R., Campbell, K.P., Ekblom, P., Genersch, E., 2003. Opposing roles of integrin alpha6beta1 and dystroglycan in laminin-mediated extracellular signal-regulated kinase activation. *Mol. Biol. Cell* 14, 2088–2103.
- Gerber, W.V., Yatskievych, T.A., Antin, P.B., Correia, K.M., Conlon, R.A., Krieg, P.A., 1999. The RNA-binding protein gene, hermes, is expressed at high levels in the developing heart. *Mech. Dev.* 80, 77–86.
- Harland, R.M., 1991. In situ hybridization: an improved whole-mount method for *Xenopus* embryos. *Methods Cell Biol.* 36, 685–695.
- Hayashi, Y.K., Ogawa, M., Tagawa, K., Noguchi, S., Ishihara, T., Nonaka, I., Arahata, K., 2001. Selective deficiency of alpha-dystroglycan in Fukuyama-type congenital muscular dystrophy. *Neurology* 57, 115–121.
- Heasman, J., 2002. Morpholino oligos: making sense of antisense? *Dev. Biol.* 243, 209–214.
- Henry, M.D., Campbell, K.P., 1998. A role for dystroglycan in basement membrane assembly. *Cell* 95, 859–870.
- Henry, M.D., Satz, J.S., Brakebusch, C., Costell, M., Gustafsson, E., Fassler, R., Campbell, K.P., 2001. Distinct roles for dystroglycan, beta1 integrin and perlecan in cell surface laminin organization. *J. Cell Sci.* 114, 1137–1144.
- Hino, N., Kobayashi, M., Shibata, N., Yamamoto, T., Saito, K., Osawa, M., 2001. Clinicopathological study on eyes from cases of Fukuyama type congenital muscular dystrophy. *Brain Dev.* 23, 97–107.
- Horne-Badovinac, S., Lin, D., Waldron, S., Schwarz, M., Mbamalu, G., Pawson, T., Jan, Y., Stainier, D.Y., Abdelilah-Seyfried, S., 2001. Positional cloning of heart and soul reveals multiple roles for PKC lambda in zebrafish organogenesis. *Curr. Biol.* 11, 1492–1502.
- James, M., Nuttall, A., Ilsley, J.L., Ottersbach, K., Tinsley, J.N., Sudol, M., Winder, S.J., 2000. Adhesion-dependent tyrosine phosphorylation of beta-dystroglycan regulates its interaction with utrophin. *J. Cell Sci.* 113, 1717–1726.
- Kablar, B., Vignali, R., Menotti, L., Pannese, M., Andreazzoli, M., Polo, C., Giribaldi, M.G., Boncinelli, E., Barsacchi, G., 1996. Xotx genes in the developing brain of *Xenopus laevis*. *Mech. Dev.* 55, 145–158.
- Kanagawa, M., Saito, F., Kunz, S., Yoshida-Moriguchi, T.B.R., Kobayashi, Y.M., Muschler, J., Dumanski, J.P., Michele, D.E., Oldstone, M.B., Campbell, K.P., 2004. Molecular recognition by LARGE is essential for expression of functional dystroglycan. *Cell* 25 (117(7)), 953–964.
- Kano, H., Kobayashi, K., Herrmann, R., Tachikawa, M., Many, H., Nishino, I., Nonaka, I., Straub, V., Talim, B., Voit, T., Topaloglu, H., Endo, T., Yoshikawa, H., Toda, T., 2002. Deficiency of alpha-dystroglycan in muscle–eye–brain disease. *Biochem. Biophys. Res. Commun.* 291, 1283–1286.
- Koulen, P., Blank, M., Kroger, S., 1998. Differential distribution of beta-dystroglycan in rabbit and rat retina. *J. Neurosci. Res.* 51, 735–747.
- Leu, S.T., Jacques, S.A., Wingerd, K.L., Hikita, S.T., Tolhurst, E.C., Pring, J.L., Wiswell, D., Kinney, L., Goodman, N.L., Jackson, D.Y., Clegg, D.O., 2004. Integrin alpha4beta1 function is required for cell survival in developing retina. *Dev. Biol.* 276, 416–430.
- Lewis, J.M., Baskaran, R., Taagepera, S., Schwartz, M.A., Wang, J.Y., 1996. Integrin regulation of c-Abl tyrosine kinase activity and cytoplasmic-nuclear transport. *Proc. Natl. Acad. Sci. U. S. A.* 93 (26), 15174–15179.
- Li, M., Sakaguchi, D.S., 2002. Expression patterns of focal adhesion associated proteins in the developing retina. *Dev. Dyn.* 225, 544–553.
- Li, M., Sakaguchi, D.S., 2004. Inhibition of integrin-mediated adhesion and signaling disrupts retinal development. *Dev. Biol.* 275, 202–214.
- Li, M., Babenko, N.A., Sakaguchi, D.S., 2004. Inhibition of protein tyrosine kinase activity disrupts early retinal development. *Dev. Biol.* 266, 209–221.
- Libby, R.T., Champlaud, M.F., Claudepierre, T., Xu, Y., Gibbons, E.P., Koch, M., Burgeson, R.E., Hunter, D.D., Brunken, W.J., 2000. Laminin

- expression in adult and developing retinae: evidence of two novel CNS laminins. *J. Neurosci.* 20, 6517–6528.
- Lunardi, A., Dente, L., 2002. Molecular cloning and expression analysis of dystroglycan during *Xenopus laevis* embryogenesis. *Mech. Dev.* 119, S49–S54.
- Michele, D.E., Barresi, R., Kanagawa, M., Saito, F., Cohn, R.D., Satz, J.S., Dollar, J., Nishino, I., Kelley, R.I., Somer, H., Straub, V., Mathews, K.D., Moore, S.A., Campbell, K.P., 2002. Post-translational disruption of dystroglycan-ligand interactions in congenital muscular dystrophies. *Nature* 418, 417–422.
- Moore, S.A., Saito, F., Chen, J., Michele, D.E., Henry, M.D., Messing, A., Cohn, R.D., Ross-Barta, S.E., Westra, S., Williamson, R.A., Hoshi, T., Campbell, K.P., 2002. Deletion of brain dystroglycan recapitulates aspects of congenital muscular dystrophy. *Nature* 418, 422–425.
- Muntoni, F., Brockington, M., Blake, D.J., Torelli, S., Brown, S.C., 2002. Defective glycosylation in muscular dystrophy. *Lancet* 360, 1419–1421.
- Nieuwkoop, P.D., Faber, J., 1967. *Normal Table of Xenopus laevis*. Daudin, North Holland, Amsterdam.
- Pannese, M., Polo, C., Andreazzoli, M., Vignali, R., Kablar, B., Barsacchi, G., Boncinelli, E., 1995. The *Xenopus* homologue of *Otx2* is a maternal homeobox gene that demarcates and specifies anterior body regions. *Development* 121, 707–720.
- Pujic, Z., Malicki, J., 2004. Retinal pattern and the genetic basis of its formation in zebrafish. *Semin. Cell Dev. Biol.* 15, 105–114.
- Scheele, S., Falk, M., Franzen, A., Ellin, F., Ferletta, M., Lonaio, P., Andersson, B., Timpl, R., Forsberg, E., Ekblom, P., 2005. Laminin {alpha}1 globular domains 4–5 induce fetal development but are not vital for embryonic basement membrane assembly. *Proc. Natl. Acad. Sci. U. S. A.* 102, 1502–1506.
- Schmitz, F., Drenckhahn, D., 1997. Dystrophin in the retina. *Prog. Neurobiol.* 53, 547–560.
- Toda, T., Kobayashi, K., Kondo-Iida, E., Sasaki, J., Nakamura, Y., 2000. The Fukuyama congenital muscular dystrophy story. *Neuromuscul. Disord.* 10, 153–159.
- Viczian, A.S., Vignali, R., Zuber, M.E., Barsacchi, G., Harris, W.A., 2003. *XOtx5b* and *XOtx2* regulate photoreceptor and bipolar fates in the *Xenopus* retina. *Development* 130, 1281–1294.
- Wary, K.K., Mariotti, A., Zurzolo, C., Giancotti, F.G., 1998. A requirement for caveolin-1 and associated kinase Fyn in integrin signaling and anchorage-dependent cell growth. *Cell* 94 (5), 625–634.
- Williamson, R.A., Henry, M.D., Daniels, K.J., Hrstka, R.F., Lee, J.C., Sunada, Y., Ibraghimov-Beskrovnaya, O., Campbell, K.P., 1997. Dystroglycan is essential for early embryonic development: disruption of Reichert's membrane in *Dag1*-null mice. *Hum. Mol. Genet.* 6, 831–841.
- Winder, S.J., 2001. The complexities of dystroglycan. *Trends Biochem. Sci.* 26, 118–124.
- Zuber, M.E., Gestri, G., Viczian, A.S., Barsacchi, G., Harris, W.A., 2003. Specification of the vertebrate eye by a network of eye field transcription factors. *Development* 130, 5155–5167.